Characteristics and properties of metal aluminum thin films prepared by electron cyclotron resonance plasma-assisted atomic layer deposition technology*

Xiong Yu-Qing(熊玉卿)[a], Li Xing-Cun(李兴存)[b], Chen Qiang(陈 强)[b]†, Lei Wen-Wen(雷雯雯)[b], Zhao Qiao(赵 桥)[b], Sang Li-Jun(桑利军)[b], Liu Zhong-Wei(刘忠伟)[b], Wang Zheng-Duo(王正铎)[b], and Yang Li-Zhen(杨丽珍)[b]

[a] *Science and Technology on Surface Engineering Laboratory, Lanzhou Institute of Physics, Lanzhou* 730000, *China*
[b] *Laboratory of Plasma Physics and Materials, Beijing Institute of Graphic Communication, Beijing* 102600, *China*

(Received 24 November 2011; revised manuscript received 13 January 2012)

Metal aluminum (Al) thin films are prepared by 2450 MHz electron cyclotron resonance plasma-assisted atomic layer deposition on glass and p-Si substrates using trimethylaluminum as the precursor and hydrogen as the reductive gas. We focus our attention on the plasma source for the thin-film preparation and annealing of the as-deposited films relative to the surface square resistivity. The square resistivity of as-deposited Al films is greatly reduced after annealing and almost reaches the value of bulk metal. Through chemical and structural analysis, we conclude that the square resistivity is determined by neither the contaminant concentration nor the surface morphology, but by both the crystallinity and crystal size in this process.

Keywords: aluminum, plasma-assisted atomic layer deposition, annealing

PACS: 81.15.Gh, 07.57.Ty, 07.79.Lh, 07.85.Jy **DOI:** 10.1088/1674-1056/21/7/078105

1. Introduction

Aluminum (Al) and its alloy thin films (∼100 nm) will be widely used for interconnections in both bipolar and metal-oxide-semiconductor integrated circuit devices,[1,2] device envelopment,[3−5] and waveguides.[6] As the minimal feature size shrinks below nano-size, successful Al metallization becomes a critical process, especially in memory devices. Physical vapour deposition (PVD) techniques such as evaporation and sputtering are often used to deposit Al films for these applications due to their high deposition rates and successful processing protocol. However, the deposition of a uniform thin Al film becomes extremely difficult with a high trench aspect ratio. Conventional line-of-sight PVD techniques yield insufficient step coverage. Therefore, the simple Al evaporation/sputtering method cannot be applied to a high aspect ratio of trench metallization because of its poor hole-filling characteristics and unconformality, even though as-deposited Al films show a high conductivity close to the ideal bulk value.[7−10] As an alternative to PVD, chemical vapour deposition (CVD) has received considerable attention because of its sufficiently conformal coverage and relatively low process temperature. However, the high surface roughness obtained from CVD-deposited Al film has been generally unsatisfactory, in particular when the thickness of the film is of the order of 5–10 nm. The island growth mode causes void formation in the initial stage of Al film growth.

Atomic layer deposition (ALD) is a variation of CVD, in which there is an alternating supply of the gaseous precursors to the substrate.[11,12] Chemisorption through alternating pulses of purge precursor and reactive gas in the ALD process reveals that the deposited film has good conformality, and is independent of the substrate configuration. In addition, in ALD, the self-limiting growth of the film can be achieved, leading to uniformity over a large area.[13] This means that in ALD the thin Al film can be uniformly deposited in a trench with a high trench aspect ratio.

*Project supported by the National Natural Science Foundation of China (Grant No. 11175024), the Beijing Natural Science Foundation, China (Grant No. 1112012), the Science and Technology on Surface Engineering Laboratory, and the Beijing Education Committee, China (Grant Nos. BM201002, 2011BAD24B01, KM201110015008, KM201010015005, and PHR20110516).

†Corresponding author. E-mail: lppmchenqiang@hotmail.com

© 2012 Chinese Physical Society and IOP Publishing Ltd

It is well known that plasma-assisted atomic layer deposition (PA–ALD) always achieves a higher growth rate and lower growth temperature than thermal ALD (T-ALD). Thus in this paper, we explore the characteristics of Al thin films deposited on glass and p-Si substrates by PA–ALD. We employ plasma generated by electron cyclotron resonance (ECR) at a microwave frequency of 2450 MHz to enhance ALD. The plasma generated by ECR enhances the surface uniformity and thickness control in PA–ALD because this source can provide a remote plasma and produce a high-density species under low pressure. No electrode of this source prevents pollution from the sputtered electrode materials. Although substrate damage from ion collisions is not of major concern,[14] this phenomenon is unavoidable in capacitively coupled plasma.[15,16] Then, Al films with a flat surface and small square resistivity are expected to be obtained in ECR PA–ALD.

We also perform annealing for high conductivity in this work. As a result, the excellent qualities of Al thin films after annealing change the concept and indicate that crystallinity and crystal size, rather than contaminant concentration, determine the square resistivity.

2. Experimental details

We chose two kinds of substrates, i.e., glass and p-Si, on which the Al thin films were grown. The substrates were used for different purposes: structure analysis and property measurement. Normally the resistivity measurement was carried out on glass substrate rather than p-Si to avoid the intrinsic resistivity from doped Si. However, we used Fourier transform infrared (FTIR) on the p-Si substrate to analyse the chemical structure. To obtain a hydrogen-terminated surface, we dipped the glass and p-Si substrates in a diluted HF (HF:H_2O=1:100) solution and then rinsed them in de-ionized water for pretreatment several times.

In Al deposition we used liquid trimethylaluminum (TMA) as an Al precursor and H_2 as the reductive gas. During processing the TMA was carried by Ar gas at 20 sccm, while the H_2 flowed at 100 sccm. The pulsed purge times of the Al source, H_2, and Ar were 2.5 s, 15 s, and 5 s, respectively, after optimality. The total cycle then consisted of TMA (2.5 s)/Ar (5 s)/H_2(15 s)/Ar (5 s).

Regardless of the effect of power on the conductivity of an as-deposited-Al thin film, the ECR plasma powers were tuned from 50 to 250 W, and the temperature varied from room temperature to 350 °C.

For comparison, the Al films were prepared using both PA–ALD and plasma-enhanced chemical vapor deposition (PECVD). For PA–ALD we used both the radio frequency (RF) and ECR plasma sources to deposit the Al thin film. There are two processes in RF PA–ALD, i.e., the plasma was switched on during the H_2 purge and the whole deposition period. In ECR PA–ALD, however, the plasma was switched on only for the whole deposition period. For PECVD, no alternately pulsed purging of TMA and H_2 was carried out during deposition; instead, they were input simultaneously into the chamber for Al deposition.

It is well known that Al easily forms a native oxide when exposed to air, which is electrically insulating. Therefore, to minimize oxidation, the apparatus consisted of a deposition chamber and a load-locked preparation chamber. After Al film deposition, inert gas Ar was let into the deposition chamber as the sample cooled.

We measured the square resistivity using a four-point probe (RTS-8, 10^{-3}–10^{6} Ω/□, resolution < ±0.3%, Guangzhou, China) to evaluate the conductive properties. The film thickness with respect to the number of ALD cycles was detected with an ellipsometer (HORIBA JOBIN YVON UVISEL). We used X-ray diffraction (XRD, Rigaku D/max-200 diffractometer, Cu Kα) to obtain the crystalline pattern. An atomic force microscope (AFM, Veeco 320, USA) was used to scan the morphologies of the films deposited before and after the annealing process. We used FTIR, (Shimadzu, FTIR-8400, Japan, precision: ±4 cm^{-1}) to analyse the chemical structure related to the electrical properties.

3. Results and discussion

To compare the films deposited by ALD and PECVD, we prepared the Al thin films on glass substrates to measure the resistivity and on p-Si to measure the surface roughness. The processing parameters are listed in Table 1. From Table 1 we see that the properties of the prepared Al films depend greatly on the deposition methods. The thinnest Al film was obtained with the RF PA–ALD when the plasma was only switched on during the H_2 gas purge. The growth rate was only 0.0133 nm/cycle. A 1.04 nm/cycle deposition rate

Table 1. Thicknesses and properties of Al films under different growth conditions.

Deposition condition	RF plasma on H_2 ALD	RF plasma on the whole ALD process	PECVD
power/W	100	250	250
TMA/(sccm/s)	20/4	20/4	20/0
H_2/(sccm/s)	50/8	50/8	50/0
purge Ar/(sccm/s)	30/2	30/2	–
substrate temperature/°C	250	250	RT
magnetic field/mT	6.2	6.2	6.2
deposition time	300 cycles	150 cycles	30 min
film thickness/nm	4	156.2	165.1
R_s/(kΩ/□)	43.3	12	15
RMS/nm	0.54	0.78	1.34

was achieved when the RF plasma was kept on for the whole ALD process. This means that the plasma largely determined the Al film growth rate. Comparing the square resistivities of these as-deposited films, we see that the film obtained during the whole PA–ALD had the highest conductivity. Considering the effect of film thickness, which is relevant to the resistivity, this shows that RF PA–ALD benefited low-resistivity film growth, although the value was still remarkably higher than that for the bulk Al.

A 5.5 nm/min deposition rate was achieved when the Al film was deposited through PECVD, i.e., simultaneous purging of TMA and H_2 in the chamber instead of alternating pulsed purging, as Table 1 shows. This implies that the Al film simultaneously formed in gaseous and solid phases, which certainly increased the deposition rate. Moreover, the square resistivity of the as-deposited Al film was higher than that of the film deposited by RF–PA–ALD. We assume that this is because more C- and H-related contamination in the growth-film by PECVD leads to high resistivity, which can be identified with the FTIR spectroscope in Fig. 1. The peaks at 2800–2980 cm^{-1}, assumed to be the $–CH_n$ stretching vibration modes, are higher in the PECVD film. The peak at 680 cm^{-1} corresponding to AlH_3 bond stretching in the FTIR spectrum indicates that hydrogen chemically bonded to the Al atoms and depended on the deposition method, but did not significantly affect the resistivity.

The surface roughnesses in RF–PA–ALD and PECVD were quite high, as expected from the direct interaction of the species with the substrates; thus, we tried to use remote plasma generated by an ECR source.

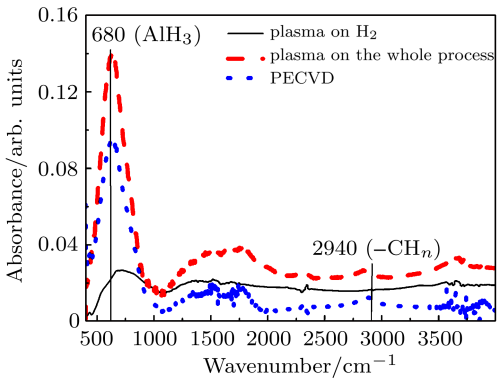


Fig. 1. (colour online) The FTIR spectra of Al film deposition in various plasma-assisted ALD processes.

As shown in Fig. 2, the film thickness increases linearly with the processing cycle when ECR PA–ALD was used for the whole process, although the ECR plasma power was increased to 250 W and the etching was considerable. This means that the Al film had self-controlled growth through the reductive reaction of the monolayer chemisorption of TMA with plasma dissociation H atoms during the pulsed purging. Based on the data in Fig. 2, the derived deposition rate is obtained to be 0.188 nm/cycle. Compared with the data in Table 1, this is remarkably higher than the rate of 0.0133 nm/cycle for only-H_2 RF–PA–ALD, but significantly lower than 1.04 nm/cycle when RF plasma assists the whole ALD process. One reason for the high growth rate is that in RF–PA–ALD, the direct interaction of the species with the substrate enhances film growth and restricts the competitive ablation reactions. The lowest deposition rate in only-H_2–RF–ALD can be explained by the low availability of H atoms in the plasma-assisted stage to reduce the chemisorptive TMA precursor density.

From the insert in Fig. 2, we further presume that the Al films prepared in ECR PA–ALD followed the island growth mode (which will be later confirmed

in AFM images). The lack of zero crossing in the thickness–versus–growth cycles in the coordination in Fig. 2 means that particle nucleation grows randomly on the surface. In previous work,[17] however, we noticed that the nucleation of particles in magnetic-field-enhanced RF–PA–ALD greatly improved layer-by-layer from the island with the growth line passing through the zero point. However, this did not happen here with ECR PA–ALD, even when a magnetic field from the coils was also generated on the substrate. The reason for this is still under investigation.

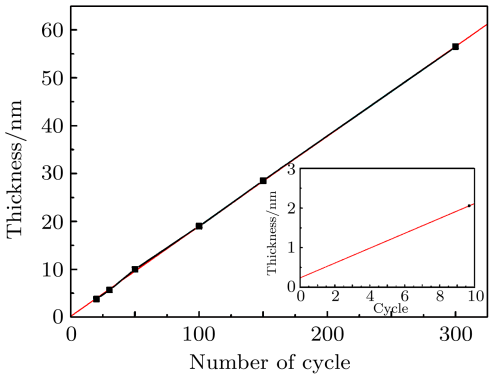


Fig. 2. (colour online) The relationship between Al film thickness and processing cycle in ECR PA–ALD (TMA 20 sccm/2.5 s). The square dots denote the experimental data, and the solid line represents a fit to the data. The insert is the partial amplification of the curve.

We then studied, in detail, the influence of ECR plasma power on the deposition rate, and the results are shown in Fig. 3(a). We see that the remote plasma causes a new film growth mode other than the one generated by the directly interacting plasma in the RF plasma.[15,16] Here, the higher the ECR power, the thicker the film grows.

Figure 3(b) confirms the self-controlled growth mode with the monolayer chemisorption of TMA by varying the TMA pulse time. The sequence consisted of TMA exposure for 1–5 s and Ar purging for 5 s, followed by exposure to H_2 for 15 s, and then Ar purging for 5 s. In Fig. 3(b) we see that the growth rate increases as the TMA pulse time increases to around 3 s and then becomes constant at about 0.19 nm per cycle with a 5 s pulse time. These results suggest that a typical self-limiting chemisorption of TMA occurs in ECR PA–ALD Al even when the plasma is switched on for the whole process, and that the TMA pulsed purge period is not less than 2 s in this system.

The influence of substrate temperature on the Al film growth rate displayed in Fig. 4(a) shows that Al film growth in ECR PA–ALD is in the chemisorptive

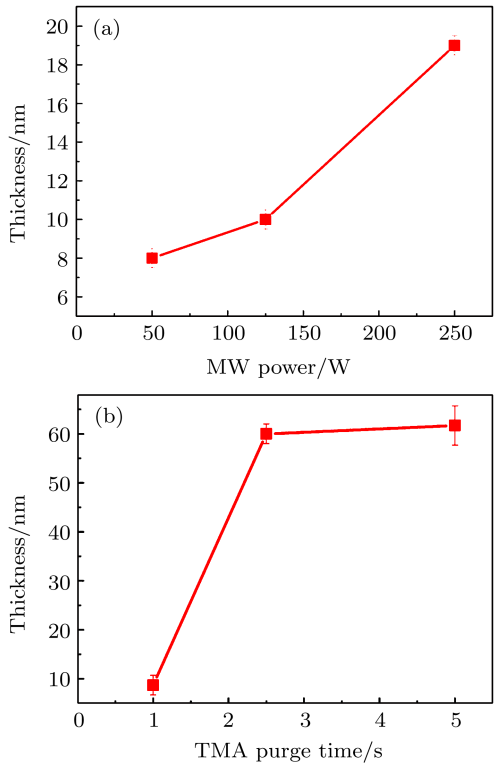


Fig. 3. (colour online) Al film thicknesses versus (a) MW power and (b) TMA pulsed purge period.

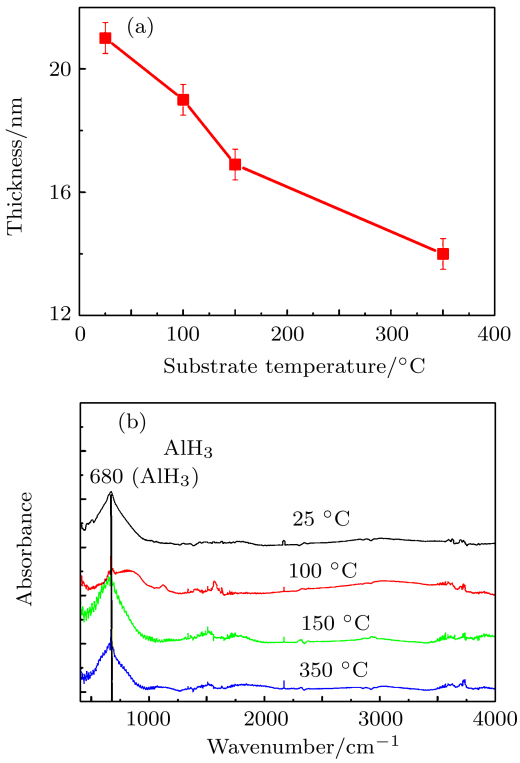


Fig. 4. (colour online) Influences of substrate temperature on (a) the growth rate of Al films, and (b) the FTIR spectra.

mode. The decay of film thickness with the substrate temperature increasing shows that the desorption of

the physisorption precursor from the substrate occurs at high temperature.

From the FTIR spectrum in Fig. 4(b), we conclude that the ECR remote plasma is conductive to restriction on contamination in the film. The peaks at 2800–2980 cm^{-1}, assumed to be the $–CH_n$ stretching vibration modes, are negligible in the spectrum. However, the similarity in the spectrum of as-deposited film at various deposition temperatures implies that the chemical structure in this spectrum cannot reveal the intrinsic properties of an Al film, such as conductivity. The AlH_3 peak observed in all samples, even at a high substrate temperature of 350 °C, does not alone reasonably explain the big difference in square resistivity seen in Table 2. All the as-deposited films show a high resistivity, although the sample prepared at 350 °C shows an infinite resistivity because of the no/random chemisorption that occurs at such a temperature.

Table 2. The resistivities and thickness of films dependent on the substrate temperature.

Substrate temperature/°C	Square resistivity R_s/(kΩ/□)	
	before annealing	after annealing
25 (21 nm/100 cycle)	43.3	0.050
100 (19 nm/100 cycle)	36.5	0.048
150 (17 nm/100 cycle)	45.6	0.049
350 (14 nm/100 cycle)	–	–

After annealing at 250 °C for 10 min, on the other hand, the conductivities were greatly improved. We obtained square resistivities of 48 Ω/□, 49 Ω/□, and 50 Ω/□ for film thicknesses of 21 nm, 19 nm, and 17 nm, respectively. Based on the negligible changes in the FTIR spectrum before and after annealing (Fig. 4(b)), we predict that the square resistivity of Al films prepared by ECR PA–ALD might not be dominated by the chemical structure. Other factors such as surface morphology or crystallinity might play an essential role.

The AFM images in Fig. 5 show that the crystal size of Al films after annealing influences the square resistivity. Before annealing, the root mean square (RMS) of the grain size is 0.773 nm for as-deposited films, but after annealing the RMS of the grain size arrives at 1.4 nm (the RMS of the grain size of the glass substrate is 1.21 nm). The Al crystal size was obviously enlarged after annealing, from an average of 71.67 nm to 127.67 nm, as determined from the images. The large crystal size minimizes the crystal interface, which leads to the small electron transfer resistivity.[18]

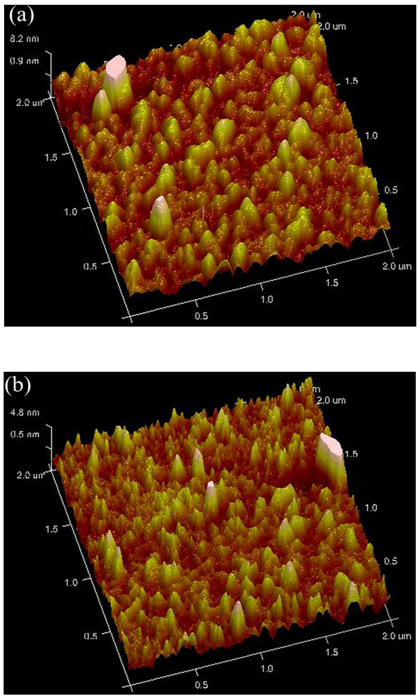


Fig. 5. (colour online) Morphologies of (a) as-deposited Al (deposited at 150 °C, 40 cycles), and (b) after annealing at 250 °C for 10 min.

Additionally, from the AFM images in Fig. 5, we infer the early stages of Al nucleation during ALD. Discrete nanoparticles at the initial stage of ECR PA–ALD grow and coalesce into the film with an increasing number of ALD cycles. The films are fine-grained, highly conformal, and ultimately form a continuous layer after ∼40 cycles. However, the aggregated nanograins coalesce into cylinders in crystal style only with annealing.

The Al crystal growth after annealing was identified by the XRD pattern (Fig. 6). Before annealing, the signal corresponding to the crystal phase was veiled by the background noise, but after annealing obvious planes (111), (200), (200), and (311) in the pattern appeared. This is a typical face-centre-cubic (fcc) Al crystal compared with the standard card (No. 65-2869).

Concerning the square resistivity, we deduce from the AFM images and XRD pattern that when Al films were deposited in ECR PA–ALD, the small particles were nucleated in island mode on the glass substrate due to the remote plasma containing few charged particles in low energy and more active radicals. The

Al films normally show a selectivity growth mode dependent on the surface energy and polarity of the substrate. The island growth mode causes the as-deposited films to be in an un-continuous state, which leads to a high resistivity when the nucleated particles aggregate and form the film with nano-scale thickness. This might be the reason why the square resistivity of the film is independent of the deposition temperature, as shown in Table 2. In Table 2 we also notice that the resistivity of the sample prepared at a substrate temperature of 150 °C is 45.6 kΩ/□, a little higher than that of film grown at room temperature (43.3 kΩ/□). However, the momentum of the nucleated grain immigration is obtained during annealing, which promotes crystal formation and growth. The relatively small concentration of amorphous Al and relevant C and H contaminations after crystallization still obstruct electron mobility. The square resistivity of 40 Ω/□ after annealing, much larger than that of the Al bulk, reminds us that two issues should be considered: one is that the film thickness needs to be greater than 100 nm, which is the critical thickness for low resistivity;[15] and the other is contamination, especially the oxide formation in the Al bulk. The photos in Fig. 7 confirm that the weak-metallic polish of Al on the glass substrates implies oxidation on the film. The Al surface was easily oxidized because the Al film was not protected before being taken out of the chamber.[15,16]

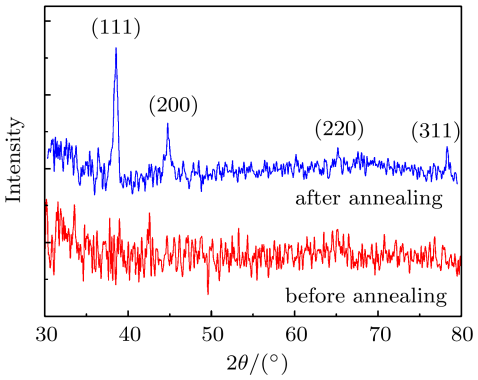


Fig. 6. (colour online) XRD patterns of as-deposited Al films before and after annealing at 250 °C for 10 min.

One way to reduce film oxidation is to anneal the film in the H_2 environment, where the O_2 adsorbed on the film surface is reduced by H atoms after annealing.[19] The C contamination in the film (normally about 3% C contained in ALD films) can also be reduced by H during annealing. Another way is to protect the surface with anti-oxidization coatings, such as TiN.[15,16] However, this restricts the use of the Al film as a conductor layer.

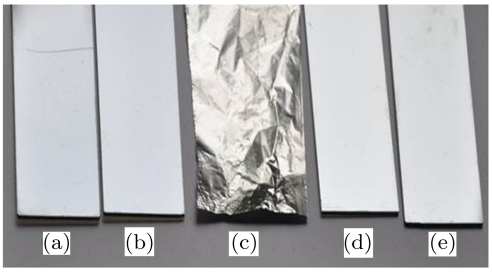


Fig. 7. (colour online) Photos of ECR–ALD Al films deposited on glass substrates under the conditions: (a) ambient temperature, H_2 at 100 sccm/15 s, R_s = 48 Ω/□, thickness = 21 nm; (b) 100 °C, H_2 at 100 sccm/15 s, R_s = 49 Ω/□, thickness = 19 nm; (c) Al foil; (d) 150 °C, H_2 at 100 sccm/15 s, R_s = 69 Ω/□, thickness = 16.9 nm; (e) 100 °C, H_2 at 100 sccm/25 s, R_s = 45 Ω/□, thickness = 25.8 nm.

4. Conclusions

Metal Al films were deposited by PA–ALD, and Al films were also deposited by PECVD for comparison. The result shows that Al metal films can be deposited by all the methods mentioned above, but the chemical structure, square resistivity, and morphology are related to the assistant methods. PA–ALD provides a better-property metal; in particular, the ECR remote plasma can deposit a relatively pure film. The chemical structure does not seem to dominate the conductivity but rather the crystallinity, which significantly determines electron mobility. The result is that annealing is very important for achieving low Al resistivity. The enlarged crystal size and low contaminations after annealing are responsible for the enhanced conductivity.

References

[1] Amazawa T 1998 *J. Electrochem. Soc.* **145** 4327
[2] Amazawa T, Yamamoto E and Arita Y 1998 *IEEE Trans. Electron Devices* **45** 815
[3] Zhang J, Yang D and Ou X 2008 *Trans. Nonferrous Met. Soc. China* **18** 312
[4] Wu G 2007 *Mater. Lett.* **61** 3815
[5] Wu S K, Yen S C and Chou T S 2006 *Surf. Coat. Tech.* **200** 2769
[6] Barber J P, Conkey D B, Lee J R, Hubbard N B, Howell L L, Yin D, Schmidt H and Hawkins A R 2005 *IEEE Photon. Technol. Lett.* **17** 363
[7] Cooke M J, Heinecke R A, Stern R C and Maes J W C 1982 *Solid State Technol.* **25** 62
[8] Green M L, Levy R A, Nuzzo R G and Coleman E 1984 *Thin Solid Films* **114** 367

[9] Kim D H and Kim B Y 2001 *J. Electrochem. Soc.* **148** C10

[10] Huang Y, Gou H Y, Liao Z W, Sun Q Q, Zhang W and Ding S J 2010 *Acta Phys. Sin.* **59** 2057 (in Chinese)

[11] Leskela M, Niinisto L, Suntola T and Simpson M 1990 *Atomic Layer Epitaxy* (Glasgow: Blackie and Son Ltd) p. 1

[12] Suntola T and Hurle D T J 1994 *Handbook of Crystal Growth* (Elsevier, Amsterdam) p. 601

[13] Ritala M, Leskelae M, Dekker J P, Mutsaers C, Soininen P J and Skarp J 1999 *Chem. Vap. Deposition* **5** 7

[14] Diatezua D M, Wang Z, Park D, Chen Z, Rockett A and Morkoc H 1998 *J. Vac. Sci. Technol.* **16** 2

[15] Lee Y J and Kang S W 2002 *Electrochem. Solid-State Lett.* **5** C91

[16] Lee Y J and Kang S W 2002 *J. Vac. Sci. Technol.* A **20** 1983

[17] Li X C 2011 *The Role of Magnetic Field on PA–ALD Al_2O_3 Thin film* (MS Thesis) (Beijing: Beijing Institute of Graphic Communication) (in Chinese)

[18] Fischer J E, Dai H, Thess A, Lee R, Hanjani N M, Dehaas D L, and Smalley R E 1997 *Phys. Rev.* B **55** R4921

[19] Aaltonen T 2005 *Atomic Layer Deposition of Noble Metal Thin Films* (PhD dissertation) (Helsinki: the University of Helsinki)